Spectroscopic Evidence for an Oxazolone Structure of the b_2 Fragment Ion from Protonated Tri-Alanine

Jos Oomens,[a] Sarah Young,[b] Sam Molesworth,[b] and Michael van Stipdonk[b]

[a] FOM Institute for Plasma Physics Rijnhuizen, Nieuwegein, The Netherlands
[b] Department of Chemistry, Wichita State University, Wichita, Kansas, USA

Infrared multiple photon dissociation (IRMPD) spectroscopy is used to identify the structure of the b_2^+ ion generated from protonated tri-alanine by collision induced dissociation (CID). The IRMPD spectrum of b_2^+ differs markedly from that of protonated cyclo-alanine-alanine, demonstrating that the product is not a diketopiperazine. Instead, comparison of the IRMPD spectrum of b_2^+ to spectra predicted by density functional theory provides compelling evidence for an oxazolone structure protonated at the oxazolone N-atom. (J Am Soc Mass Spectrom 2009, 20, 334–339) © 2009 Published by Elsevier Inc. on behalf of American Society for Mass Spectrometry

Because tandem mass spectrometry (MS/MS) and collision induced dissociation (CID) are essential tools for protein identification in proteomics, a clear understanding of peptide ion dissociation/fragmentation mechanisms is essential to optimize bioinformatics approaches for rapid and accurate identification. Theoretical and experimental evidence exist for a mix of protonation sites on gas-phase peptides, including the amino-terminus, amide carbonyl oxygen atoms [1, 2], and the side chains of histidine, lysine, or arginine. Fragmentation during low-energy CID primarily involves rearrangement reactions [3–12] in which the added proton migrates from the most basic site to the amide bond that is cleaved. This general idea makes up the "mobile-proton" model of peptide dissociation [13–25], which has been augmented in the more recent "pathways in competition" model [26] including more comprehensive pre- and postdissociation processes as well as the energies of reactive configurations, intermediates, and transition states.

Knowledge of structures, particularly for product ions, is necessary to fully resolve the mechanisms behind peptide dissociation. Early experimental studies suggested that the C-terminus-containing y fragments are simple truncated peptides [6, 27, 28]. While the complementary, N-terminus-containing b species were originally thought to be acylium ions [29], it is now generally accepted they instead have a five-membered oxazolone ring structure [4, 5].

An alternative b ion structure, particularly for b_2^+, would be a six-membered diketopiperazine ring formed by nucleophilic attack on an amide carbonyl C atom by the N-terminal amino group. Neutralization-reionization experiments by Wesdemiotis and coworkers [28] provided evidence that the neutral eliminated from protonated tri-alanine to furnish y_1^+ can adopt a diketopiperazine structure. However, similar experiments showed that the b_2^+ species, which is the complementary fragment to y_1^+ generated by cleavage of the same amide bond, is not a diketopiperazine. Further evidence against a diketopiperazine structure for b_2^+ ions was obtained by comparing CID spectra generated from the b_2^+ fragment of GLG with those generated from cyclo-GL [6].

Formation of b_2^+ from tri-glycine either as an oxazolone or a diketopiperazine was studied in great detail by Paizs and Suhai using density functional theory (DFT) calculations and RRKM modeling [9, 30]. Formation of a diketopiperazine ring from protonated tri-glycine was found to involve a *trans-cis* isomerization of the N-terminal amide bond that is energetically feasible under the conditions typical of CID [9]. The other *cis* amide bond within the diketopiperazine is a product of the nucleophilic attack cleaving the amide bond. The *cis* isomer was found to lie very close to the all-*trans* isomer, which is the global minimum for the protonated peptide. The energetics for the diketopiperazine and oxazolone pathways were compared directly [30], and the barrier, relative to the ground state, was found to be significantly higher (ca. 10 kcal/mol) for the diketopiperazine pathway, although the relative energies of the two products are comparable. In addition, it was proposed that the diketopiperazine pathway may be kinetically controlled due to the

Address reprint requests to Dr. J. Oomens, FOM Institute for Plasma Physics, Edisonbaan 14, Nieuwegein 3439MN, The Netherlands. E-mail: joso@rijnhuizen.nl Or to M. van Stipdonk, Department of Chemistry, Wichita State University, Wichita, KS 67260, USA. E-mail: Mike.VanStipdonk@wichita.edu

1044-0305/09/$32.00
doi:10.1016/j.jasms.2008.10.012

Published online November 1, 2008
Received August 18, 2008
Revised October 13, 2008
Accepted October 13, 2008

trans-cis isomerization, which likely makes formation of the six-membered ring product unfavorable.

Within the context of determining peptide fragment ion structures, infrared multiple photon dissociation (IRMPD) spectroscopy has been used to characterize fragment ions from protonated peptides. For example, it was shown that b_4^+ from protonated leucine-enkephalin has an oxazolone structure [11, 12]. In addition, McLafferty rearrangement was used to generate the free-acid forms of the nicotinyl-glycine-*tert*-butyl ester and betaine-glycine-*tert*-butyl ester through transfer of an H atom and elimination of butane [31]. Comparison of the IRMPD and theoretical spectra for different isotopically-labeled isomers showed that the H atom is situated at the C-terminal acid group, and migration to amide positions is negligible on the time scale of the experiment.

Here we use IRMPD spectroscopy to unambiguously assign the structure of the b_2^+ fragment ion from protonated tri-alanine, and to compare the IR spectrum of b_2^+ to that of cyclo-alanine-alanine, and thus provide the first direct spectroscopic comparison. The experimental IR spectra are complemented by DFT calculations, which give relative energies and predicted vibrational frequencies of potential oxazolone and diketopiperazine structures. The IR spectra unambiguously identify the b_2^+ ion as an oxazolone structure and provide valuable vibrational signatures for protonated oxazolones and diketopiperazines that may be useful in future studies of peptide fragments by IRMPD spectroscopy.

Experimental

IRMPD Spectroscopy

Infrared spectra were obtained by IRMPD spectroscopy using the FTICR mass spectrometer coupled to the beamline of the free-electron-laser user facility (FELIX) in The Netherlands as described previously [32, 33]. Briefly, ions are produced by electrospray ionization (ESI) and accumulated in a hexapole ion trap. Ions are then injected into a homebuilt FTICR mass spectrometer [34], where the ion of interest is isolated and then irradiated with FELIX for 2 s at a 5 Hz repetition rate. In these experiments, the wavelength of FELIX is tuned between 5.2 and 17 μm and the macropulse energy is 35 mJ. After irradiation, parent and fragment ion intensities are recorded. Data acquisition and instrument control is accomplished using a modified version of the data system and software of Heeren and coworkers [35].

Tri-alanine and cyclo-dialanine (alanine anhydride, 3,6-dimethyl-2,5-piperazinedione) were used as 1 mM solutions in 80/20 methanol/water with ~1% acetic acid added to aid protonation. ESI of the cyclo-dialanine solution yields an abundant protonated cyclo-dialalanine at *m/z* 143. Similarly, a strong *m/z* 232 peak is generated using the tri-alanine solution. By adjusting the rf amplitude and the axial trapping voltage of the accumulation hexapole, conditions can be made such that the b_2^+ ion (*m/z* 143) is formed by CID.

Upon resonant infrared irradiation with FELIX, protonated cyclo-dialanine fragments into *m/z* 115, 98, and 44, presumably corresponding to loss of CO, to loss of CO and NH_3, and to $H_2N^+ = CH(CH_3)$, respectively. The fragment intensities are summed and divided by the total ion intensity at each wavelength to generate an IRMPD spectrum. Under similar irradiation conditions, the b_2^+ fragment of protonated AAA dissociates into *m/z* 115, i.e., by the loss of CO, presumably forming the a_2^+ ion.

Density Functional Theory Calculations

The Gaussian set of programs [36] is used for all DFT calculations. A range of protonated oxazolone and diketopiperazine structures are initially (fully) optimized at the B3LYP/6-31G(d) level of theory, and then reoptimized at the B3LYP/6-31+G(d,p) and B3LYP/6-311+G(d,p) levels of theory. Because of the small size of the model systems, an intensive search of the peptide potential energy surface using molecular dynamics simulations was not deemed necessary. Relative energies for all species are calculated by correcting B3LYP/

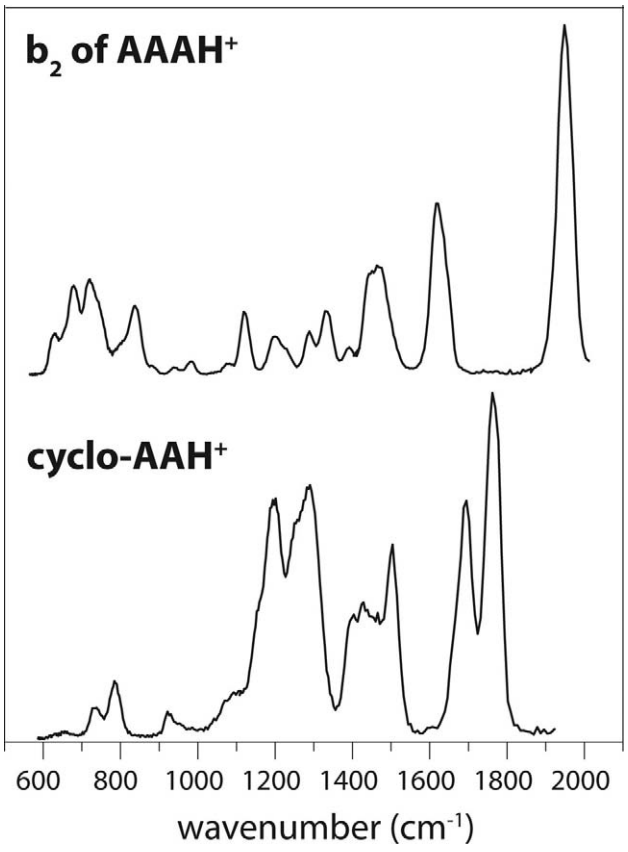

Figure 1. Comparison of the experimental IRMPD spectra recorded for the b_2^+ fragment of protonated tri-alanine and for protonated cyclo-dialanine. The large differences in the IR spectra suggest isomeric structures.

Table 1. Electronic energies, zero-point corrections, and relative energies for possible oxazolone and diketopiperazine structures for b_2^+. Electronic energies and zero-point corrections are in Hartrees. Relative energies are in kcal/mol. All values were produced at the B3LYP/6-311+g(d,p) level of theory

Structure	Energy	ZPE	E + ZPE	Rel. E
ox_1	-495.128188	0.176564	-494.951624	2.36
ox_2	-495.118188	0.176165	-494.942023	8.39
ox_3	-495.114795	0.177805	-494.93699	11.55
ox_4	-495.121278	0.17776	-494.943518	7.45
ox_5	-494.963817	0.175602	-494.788215	104.90
ox_6	-494.940618	0.173196	-494.767422	117.95
diketo_1	-495.13325	0.177859	-494.955391	0
diketo_2	-495.129922	0.177732	-494.95219	2.01
diketo_3	-495.112373	0.177808	-494.934565	13.07

6-311+G(d,p) total energies for zero-point vibrational energy (ZPE) obtained from the unscaled frequencies determined at the same level of theory. Predicted IR spectra for a range of structural isomers of the oxazolone and diketopiperazine b_2^+ species are generated at the B3LYP/6-311+g(d,p) level of theory and scaled by a factor of 0.98 for comparison to the experimental IRMPD spectra.

Results and Discussion

The experimental IRMPD spectra for protonated cyclo-AA and the b_2^+ fragment of protonated AAA (Figure 1) are very different, indicating that the two species, despite being isobaric, possess different structures. From this result alone, one can qualitatively conclude that the b_2^+ fragment of $AAAH^+$ does not have a diketopiperazine structure.

Relative energies for potential oxazolone and diketopiperazine structures are provided in Table 1. The lowest energy isomer is an O-protonated diketopiperazine, **diketo_1**. A second O-protonated isomer, **diketo_2**, differing only in the NCOH dihedral angle, and a N-protonated isomer, **diketo_3**, are 2.01 and 13.07 kcal/mol higher in energy, respectively. The lowest energy oxazolone isomer, **ox_1**, which is protonated at the ring N atom, lies 2.36 kcal/mol higher than **diketo_1**. A second oxazolone ring protonated structure (**ox_2**), and two amino N-protonated isomers, **ox_3** and **ox_4**, lie 8.39, 11.55, and 7.45 kcal/mol higher in energy, respectively. Additional ring O-protonated oxazolone structures (not shown) are more than 100 kcal/mol higher in energy than **diketo_1** and are thus ruled out as probable isomers for b_2^+.

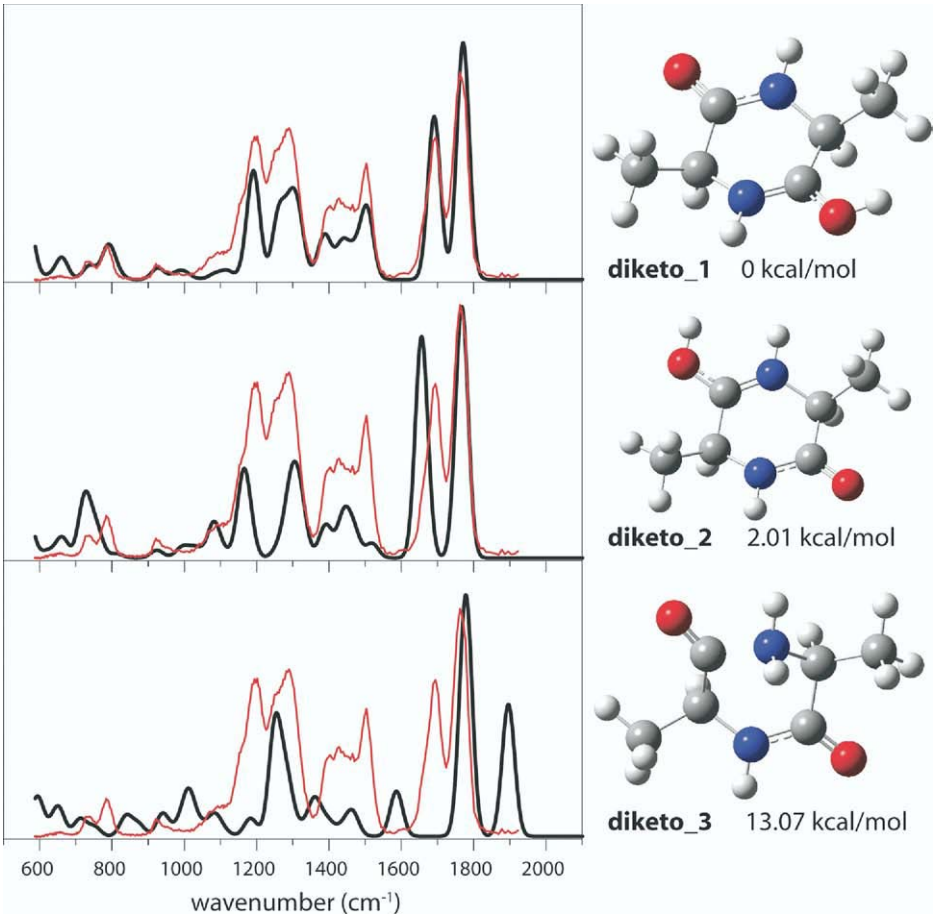

Figure 2. Experimental IRMPD spectrum of protonated cyclo-AA compared with calculated spectra for three low-energy structures. The match with the 0 kcal/mol conformer is excellent.

Figure 2 shows the experimental IRMPD spectrum of protonated cyclo-AA compared with calculated spectra for the three lowest energy diketopiperazine structures. As noted above, protonation of the diketopiperazine at one of the carbonyl oxygen atoms is preferred over protonation at the amide nitrogen atom by more than 10 kcal/mol. The spectra predicted for the two O-protonated structures are very similar. Apart from small differences in relative band intensities, the main difference is the small shift in the band between 1650 and 1700 cm^{-1}, which has mainly amide CN stretching character. In addition, the predicted spectra show differences in the weak bands between 600 and 800 cm^{-1}. These modes are mainly attributed to various NH and CH-bending modes. Despite the spectral differences being so small, the experimental spectrum unambiguously identifies the lowest energy **diketo_1** structure as the actual one. The overall agreement of experiment and theory is excellent, both in band positions and in relative intensities.

As qualitatively concluded from Figure 1, the b_2^+ fragment of protonated AAA does not have a protonated diketopiperazine structure. Hence we compare our IRMPD spectrum with computed spectra for different oxazolone conformers (Figure 3). The top two structures are protonated at the oxazolone N atom (**ox_1** and **ox_2**), while the bottom two structures are protonated at the amino group (**ox_3** and **ox_4**). From the better match of the oxazolone C = O stretch, experimentally observed at 1950 cm^{-1}, as well as from the substantially better match in the 1400–1800 cm^{-1} range, clearly the b_2^+ fragment of $AAAH^+$ has an oxazolone structure protonated at the oxazolone N-atom. The band observed at 1620 cm^{-1} is attributed to an NH_2 scissoring mode of the unprotonated N-terminus. In the terminal N protonated species, two separated bands are predicted, which are due to the oxazolone C = N stretch mode and wagging of the NH_3^+ protonated N-terminus. It is interesting to note that the b_4^+ fragment ion from Leu-enkephalin was spectroscopically determined to be

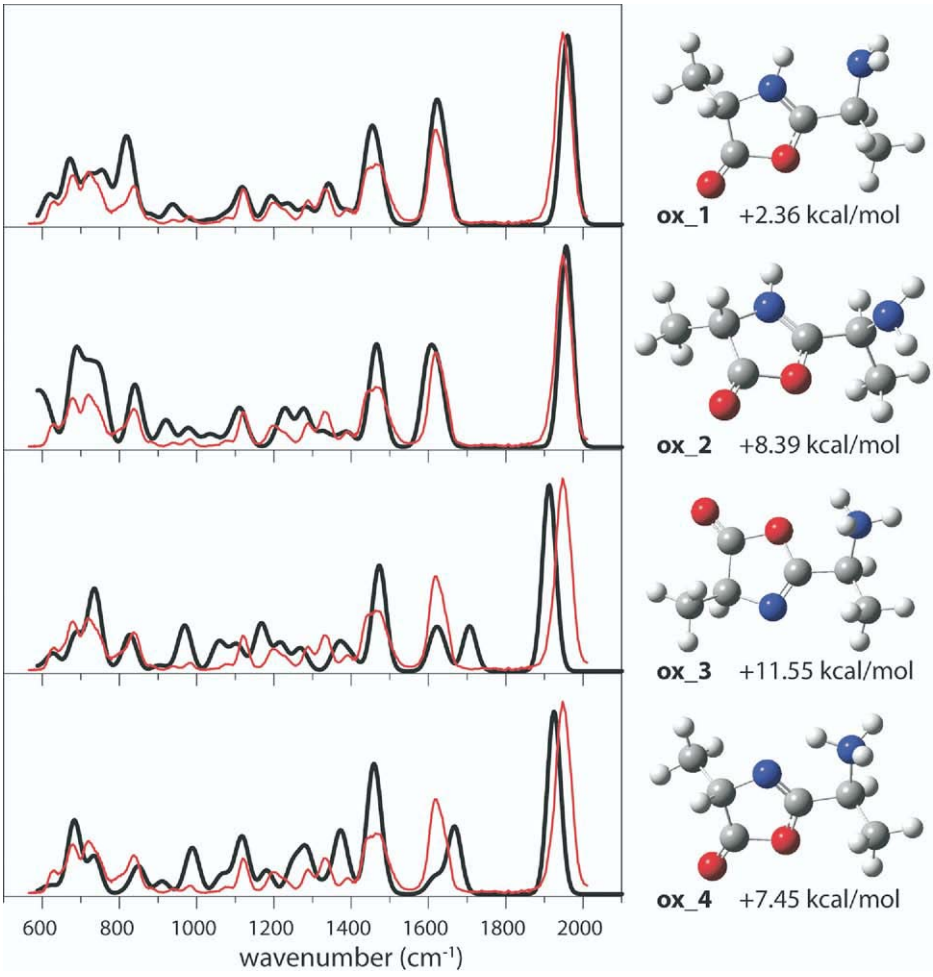

Figure 3. Experimental IRMPD spectrum of the b_2^+ fragment of protonated AAA compared with calculated spectra for four low-energy oxazolone structures. Energies are given relative to that of the lowest energy cyclo-AA isomer. The excellent match between experiment and theory for the **ox_1** structure leaves little doubt that this b_2^+ fragment has an oxazolone structure protonated on the ring N atom.

protonated at the N-terminus and not at the oxazolone ring [11].

The two oxazolone protonated conformers **ox_1** and **ox_2**, represented in the top two panels of Figure 3, differ mainly in the torsional angle around the C–C bond connecting the oxazolone ring and the backbone. The lowest energy **ox_1** structure gains its stability from a hydrogen bond between the proton on the oxazolone nitrogen atom and the N-terminus. (Note again that energies are given relative to the lowest energy diketopiperazine structure, which represents the global minimum for the *m/z* 143 isomers.) The calculated spectra for the two oxazolone protonated conformers are very similar, and it is difficult to exclude one of them on purely spectroscopic grounds. Perhaps the lack of an experimental band at the red edge of the scan range reveals that the structure indeed contains an $NH–NH_2$ hydrogen bond between the oxazolone ring and the N-terminus. The band calculated around 600 cm^{-1} in the **ox_2** conformer is due to the free NH bending of the protonated oxazolone. In addition, the calculated energy difference of ~6 kcal/mol supports the assignment of the b_2^+ fragment ion as the **ox_1** structure.

Conclusions

IRMPD spectroscopy and DFT calculations unambiguously indicate that the b_2^+ fragment from $AAAH^+$ has an oxazolone structure protonated at the oxazolone N-atom. The experimental spectrum of protonated cyclo-alanine-alanine is assigned to an O-protonated diketopiperazine structure; even small structural details such as the NCOH dihedral angle are correctly identified in the experimental spectrum.

Formation of the oxazolone structure is consistent with earlier neutralization-reionization mass spectrometry and CID studies of tri-alanine and similar small peptides [6, 28], and with the DFT studies of Paizs and Suhai [9, 30]. We note that the experiments reported in this study involve only a small peptide. Possibly larger peptides, especially tryptic peptides, will generate b_2 ions that have alternate structures [37]. Beyond identifying the structure of b_2^+ from tri-alanine, these results provide useful benchmarks and characteristic vibrational fingerprints of oxazolone and diketopiperazine conformations for future studies.

Acknowledgments

M.V.S., S.Y., and S.M. acknowledge support in part by a grant from the National Science Foundation (CAREER-0239800). DFT calculations were performed at Wichita State University using resources of the High-Performance Computing Center (HIPECC), a facility supported by the NSF under grants EIA-0216178 and EPS-0236913 and matching support from the State of Kansas and HIPECC. J.O. acknowledges support by the Nederlandse Organisatie voor Wetenschappelijk Onderzoek (NWO). The authors gratefully acknowledge the excellent support by Dr. B. Redlich and others of the FELIX staff.

References

1. Rodriquez, C. F.; Cunje, A.; Shoeib, T.; Chu, I. K.; Hopkinson A. C.; Siu, K. W. M. Proton Migration and Tautomerism in Protonated Triglycine. *J. Am. Chem. Soc.* **2001,** *123*, 3006–3012.
2. Wu, R.; Mc Mahon, T. B. Infrared Multiple Photon Dissociation Spectroscopy as Structural Confirmation for $GlyGlyGlyH^+$ and $AlaAlaAlaH^+$ in the Gas Phase. Evidence for Amide Oxygen as the Protonation Site. *J. Am. Chem. Soc.* **2007,** *129*, 11312–11313.
3. Papayannopoulos, I. A. The Interpretation of Collision-Induced Dissociation Tandem Mass Spectra of Peptides. *Mass Spectrom. Rev.* **1995,** *14*, 49–73.
4. Yalcin, T.; Khouw, C.; Csizmadia, I. G.; Peterson, M. R.; Harrison, A. G. Why are B Ions Stable Species in Peptide Spectra? *J. Am. Soc. Mass Spectrom.* **1995,** *6*, 1165–1174.
5. Yalcin, T.; Csizmadia, I. G.; Peterson, M. B.; Harrison, A. G. The Structure and Fragmentation of B_n ($n \geq 3$) Ions in Peptide Spectra. *J. Am. Soc. Mass Spectrom.* **1996,** *7*, 233–242.
6. Nold, M. J.; Wesdemiotis, C.; Yalcin, T.; Harrison, A. G. Amide bond dissociation in protonated peptides. Structures of the N-Terminal Ionic and Neutral Fragments. *Int. J. Mass Spectrom. Ion Processes* **1997,** *164*, 137–153.
7. Paizs, B.; Lendvay, G.; Vékey, K.; Suhai, S. Formation of b_2^+ Ions from Protonated Peptides: an Ab Initio Study. *Rapid Commun. Mass Spectrom.* **1999,** *13*, 525–533.
8. Harrison, A. G.; Csizmadia, I. G.; Tang, T.-H. Structure and Fragmentation of b_2 Ions in Peptide Mass Spectra. *J. Am. Soc. Mass Spectrom.* **2000,** *11*, 427–436.
9. Paizs, B.; Suhai, S. Combined Quantum Chemical and RRKM Modeling of the Main Fragmentation Pathways of Protonated GGG. II. Formation of b_2, y_1, and y_2 Ions. *Rapid Commun. Mass Spectrom.* **2002,** *16*, 375–389.
10. Paizs, B.; Suhai, S. Towards Understanding the Tandem Mass Spectra of Protonated Oligopeptides. 1: Mechanism of Amide Bond Cleavage. *J. Am. Soc. Mass Spectrom.* **2004,** *15*, 103–112.
11. Polfer, N. C.; Oomens, J.; Suhai, S.; Paizs, B. Spectroscopic and Theoretical Evidence for Oxazolone Ring Formation in Collision-Induced Dissociation of Peptides. *J. Am. Chem. Soc.* **2005,** *127*, 17154–17155.
12. Polfer, N. C.; Oomens, J.; Suhai, S.; Paizs, B. Infrared Spectroscopy and Theoretical Studies on Gas-Phase Protonated Leu-Enkephalin and Its Fragments: Direct Experimental Evidence for the Mobile Proton. *J. Am. Chem. Soc.* **2007,** *120*, 5887–5897.
13. Jones, J. L.; Dongré, A. R.; Somogyi,. Á.; Wysocki, V. H. Sequence Dependence of Peptide Fragmentation Efficiency Curves Determined by Electrospray Ionization/Surface-Induced Dissociation Mass Spectrometry. *J. Am. Chem. Soc.* **1994,** *116*, 8368–8369.
14. Tsaprailis, G.; Nair, H.; Somogyi,. Á.; Wysocki, V. H.; Zhong, W.; Futrell, J. H.; Summerfield, S. G.; Gaskell, S. J. Influence of Secondary Structure on the Fragmentation of Protonated Peptides. *J. Am. Chem. Soc.* **1999,** *121*, 5142–5154.
15. Wysocki, V. H.; Tsaprailis, G.; Smith, L. L.; Breci, L. A. Mobile and Localized Protons: A Framework for Understanding Peptide Dissociation. *J. Mass Spectrom.* **2000,** *35*, 1399–1406.
16. Tsang, C. W.; Harrison, A. G. Chemical Ionization of Amino Acids. *J. Am. Chem. Soc.* **1976,** *98*, 1301–1308.
17. Harrison, A. G.; Yalcin, T. Proton Mobility in Protonated Amino Acids and Peptides. *Int. J. Mass Spectrom. Ion Processes* **1997,** *165*, 339–347.
18. Burlet, O.; Yang, C. Y.; Gaskell, S. J. Influence of Cysteine to Cysteic Acid Oxidation on the Collision-Activated Decomposition of Protonated Peptides: Evidence for Intraionic Interactions. *J. Am. Soc. Mass Spectrom.* **1992,** *3*, 337–344.
19. Cox, K. A.; Gaskell, S. J.; Morris, M.; Whiting, A. Role of the Site of Protonation in the Low-Energy Decompositions of Gas-Phase Peptide Ions. *J. Am. Soc. Mass Spectrom.* **1996,** *7*, 522–531.
20. Summerfield, S. G.; Whiting, A.; Gaskell, S. J. Intraionic Interactions in Electrosprayed Peptide Ions. *Int. J. Mass Spectrom. Ion Processes* **1997,** *162*, 149–161.
21. Summerfield, S. G.; Cox, K. A.; Gaskell, S. J. The Promotion of *d*-Type Ions During the Low Energy Collision-Induced Dissociation of Some Cysteic Acid-Containing Peptides. *J. Am. Soc. Mass Spectrom.* **1997,** *8*, 25–31.
22. Tang, X.; Boyd, R. K. An Investigation of Fragmentation Mechanisms of Doubly Protonated Tryptic Peptides. *Rapid Commun. Mass Spectrom.* **1992,** *6*, 651–657.
23. Tang, X.; Thibault, P.; Boyd, R. K. Fragmentation Reactions of Multiply-Protonated Peptides and Implications for Sequencing by Tandem Mass Spectrometry with Low-Energy Collision-Induced Dissociation. *Anal. Chem.* **1993,** *65*, 2824–2834.
24. Csonka, I. P.; Paizs, B.; Lendavy, G.; Suhai, S. Proton Mobility in Protonated Peptides: a Joint Molecular Orbital and RRKM Study. *Rapid Commun. Mass Spectrom.* **2000,** *14*, 417–427.
25. Paizs, B.; Csonka, I. P.; Lendvay, G.; Suhai, S. Proton Mobility in Protonated glycylglycine and N-Formylglycylglycinamide: A Combined Quantum Chemical and RKKM Study. *Rapid Commun. Mass Spectrom.* **2001,** *15*, 637–647.
26. Paizs, B.; Suhai, S. Fragmentation Pathways of Protonated Peptides. *Mass Spectrom. Rev.* **2004,** *24*, 508–548.
27. Polce, M. J.; Ren, D.; Wesdemiotis, C. Dissociation of the Peptide Bond in Protonated Peptides. *J. Mass Spectrom.* **2000,** *35*(12), 1391–1398.

28. Cordero, M. M.; Houser, J. J.; Wesdemiotis, C. The Neutral Products Formed During Backbone Fragmentations of Protonated Peptides in Tandem Mass Spectrometry. *Anal. Chem.* **1993,** *65*, 1594–1601.
29. Biemann, K. Contributions of Mass Spectrometry to Peptide and Protein Structure. *Biomed. Environ. Mass Spectrom.* **1988,** *16*, 99–111.
30. Paizs, B.; Suhai, S. Combined Quantum Chemical and RRKM Modeling of the Main Fragmentation Pathways of Protonated GGG. I. Cis-trans Isomerization Around Protonated Amide Bonds. *Rapid Commun. Mass Spectrom.* **2001,** *15*, 2307–2323.
31. Van Stipdonk, M. J.; Kerstetter, D. R.; Leavitt, C. M.; Groenewold, G. S.; Steill, J.; Oomens, J. Spectroscopic Investigation of H Atom Transfer in a Gas-Phase Dissociation Reaction: McLafferty Rearrangement of Model Gas-Phase Peptide Ions. *Phys. Chem., Chem. Phys.* **2008,** *10*, 3209–3221.
32. Oepts, D.; van der Meer, A. F. G.; van Amersfoort, P. W. The Free-Electron-Laser User Facility FELIX. *Infrared Phys. Technol.* **1995,** *36*, 297–308.
33. Polfer, N. C.; Oomens, J. Reaction Products in Mass Spectrometry Elucidated with Infrared Spectroscopy. *Phys. Chem., Chem. Phys.* **2007,** *9*, 3804–3817.
34. Valle, J. J.; Eyler, J. R.; Oomens, J.; Moore, D. T.; van der Meer, A. F. G.; von Helden, G.; Meijer, G.; Hendrickson, C. L.; Marshall, A. G.; Blakney, G. T. Free Electron Laser-Fourier Transform Ion Cyclotron Resonance Mass Spectrometry Facility for Obtaining Infrared Multiphoton Dissociation Spectra of Gaseous Ions. *Rev. Sci. Instrum.* 2005, *76*, 023103.
35. Mize, T. H.; Taban, I.; Duursma, M.; Seynen, M.; Konijnenburg, M.; Vijftigschild, A.; Doornik, C. V.; Rooij, G. V.; Heeren, R. M. A. A Modular Data and Control System to Improve Sensitivity, Selectivity, Speed of Analysis, Ease of Use, and Transient Duration in an External Source FTICR-MS. *Int. J. Mass Spectrom.* **2004,** *235*, 243–253.
36. Frisch, M. J.; Trucks, G. W.; Schlegel, H. B.; Scuseria, G. E.; Robb, M. A.; Cheeseman, J. R.; Montgomery, J. A. Jr.; Vreven, T.; Kudin, K. N.; Burant, J. C.; Millam, J. M.; Iyengar, S. S.; Tomasi, J.; Barone, V.; Mennucci, B.; Cossi, M.; Scalmani, G.; Rega, N.; Petersson, G. A.; Nakatsuji, H.; Hada, M.; Ehara, M.; Toyota, K.; Fukuda, R.; Hasegawa, J.; Ishida, M.; Nakajima, T.; Honda, Y.; Kitao, O.; Nakai, H.; Klene, M.; Li, X.; Knox, J. E.; Hratchian, H. P.; Cross, J. B.; Bakken, V.; Adamo, C.; Jaramillo, J.; Gomperts, R.; Stratmann, R. E.; Yazyev, O.; A. J.; Austin, A. J.; Cammi, R.; Pomelli, C.; Ochterski, J. W.; Ayala, P. Y.; Morokuma, K.; Voth, G. A.; Salvador, P.; Dannenberg, J. J.; Zakrzewski, V. G.; Dapprich, S.; Daniels, A. D.; Strain, M. C.; Farkas, O.; Malick, D. K.; Rabuck, A. D.; Raghavachari, K.; Foresman, J. B.; Ortiz, J. V.; Cui, Q.; Baboul, A. G.; Clifford, S.; Cioslowski, J.; Stefanov, B. B.; Liu, G.; Liashenko, A.; Piskorz, P.; Komaromi, I.; Martin, R. L.; Fox, D. J.; Keith, T.; Al-Laham, M. A.; Peng, C. Y.; Nanayakkara, A.; Challacombe, M.; Gill, P. M. W.; Johnson, B.; Chen, W.; Wong, M. W.; Gonzalez, C.; Pople, J. A. *Gaussian 03, Revision D. 01*; Gaussian, Inc.: Wallingford, CT, 2004.
37. Eckart, K.; Holthausen, M. C.; Koch, W.; Spiess, J. Mass Spectrometric and Quantum Mechanical Analysis of Gas-Phase Formation, Structure, and Decomposition of Various b_2 Ions and Their Specifically Deuterated Analogs. *J. Am. Soc. Mass Spectrom.* **1998,** *9*, 1002–1011.